

Charge Transport and Recombination in Dye-Sensitized Nanocrystalline Solar Cells

Killian Lobato, Sustainable Energy Systems, University of Lisbon

Laurie Peter, Oanh Nguyen, James Jennings, Halina Dunn, Dept. Chemistry, University of Bath

The interaction of QFL (and hence the free electron density) with the trap distribution has thus far only been explored for homogeneous distributions, e.g. measuring and modelling open-circuit photovoltage decay transients[1]. If the trap states are not recombination sites (surface states), they then play no role in describing the photostationary characteristics of a cell.

Würfel et. al. [2] measured the electron density at short-circuit. They found that the extracted charge under short-circuit conditions was equivalent to that extracted from PV decay when the voltage across the cell was c.a. 550mV, and hence concluded that at short-circuit there was a significant electron density and QFL within the film. The conclusions are similar to those obtained by O'Regan and Lenzmann [3] and Boschloo et. al.[4] These methods only estimated the internal QFL at short-circuit, although one method measured the trapped electrons directly[2], and the other measured the "residual" average voltage[4].

With the knowledge of how the QFL profile behaves for different applied biases[5], it is now possible to test in conjunction, the ideas of an exponential trap distribution[6] and the diffusive model for electron transport[7] as opposed to migratory electron transport due to electric fields.

The local trapped electron density at x is determined by the local QFL level ($E_F(x) - E_{F,redox}$). For an exponential trap distribution the trapped electron density is given by;

$$n_t(x) = N_t \exp \frac{E_F(x) - E_C}{k_B T} \quad 1$$

Figure 1 illustrates a typical set of calculated QFLs that correspond to different points on the iV curve. Typically, the QFL varies strongly for $x < 0.5 \mu m$ and then is flat throughout the film. For the rest of the film ($x > 0.5 \mu m$) the QFL does not vary until the applied bias becomes equal to the internal QFL. It is, therefore, easy to foresee that the trapped electron density in the TiO_2 will not vary significantly until the applied bias becomes equivalent to the internal QFL.

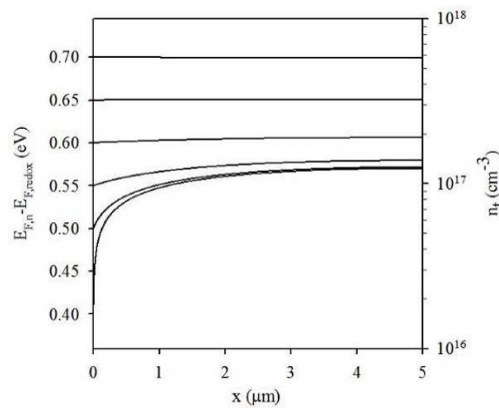


Figure 1 Example of how the QFL and the resultant trap electron density varies for different biases at $x=0$. Standard parameters were: $D_0=0.04 \text{ cm}^2 \text{ s}^{-1}$, $\tau_0=1 \text{ ms}$, $E_C - E_{F,redox}=0.95 \text{ eV}$, $N_C=10^{21} \text{ cm}^{-3}$, $N_t=10^{19} \text{ cm}^{-3}$, $T_C=1000 \text{ K}$. The density of trapped electrons is directly proportional to the QFL so only one set of curves is required to represent both.

Figure 2 demonstrates a few examples of how varying the diffusion coefficient and electron lifetime affects the QFL and the trapped electron density. The dependence on the diffusion coefficient is straightforward, whereby a lower diffusion coefficient gives rise to a higher internal QFL to support the photostationary current. This in turn gives rise to a higher trapped electron density. The electron lifetime only affects the QFL profile when $Ln < 3d$, giving rise to a maximum QFL somewhere within the film and not at $x=d$.

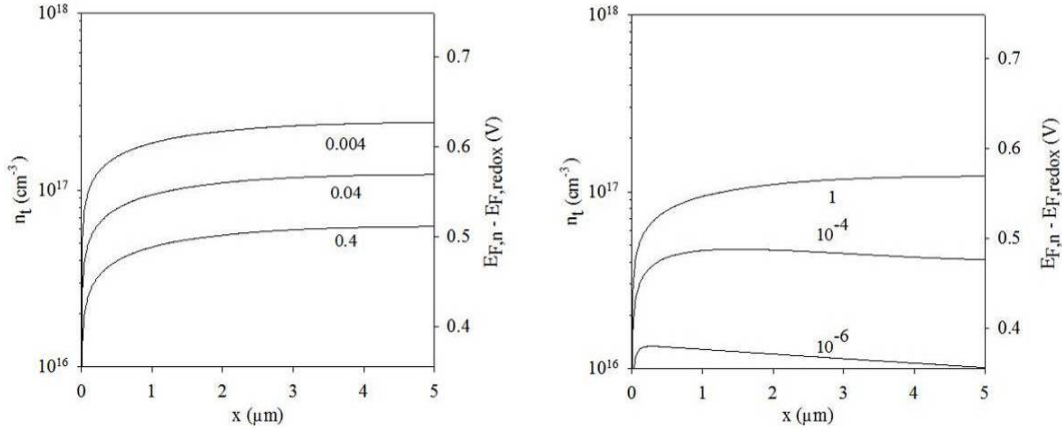


Figure 2 Left - effect of electron diffusion coefficient (cm^2s^{-1}). Right - effect of electron lifetime (ms). Standard parameters were: $D_0=0.04\text{cm}^2\text{s}^{-1}$ (right), $\tau_0=1\text{ms}$ (left), $E_C-E_{F,\text{redox}}=0.95\text{eV}$, $N_C=10^{21}\text{cm}^{-3}$, $N_t=10^{19}\text{cm}^{-3}$, $T_C=1000\text{K}$. When $L_n>3d$ the QFL profiles are independent of the electron lifetime but shift according to the diffusion coefficient. The position of the QFL only becomes a function of the lifetime when $L_n<3d$.

Having shown how the electron diffusion coefficient and lifetime affect the QFL and hence the trapped charge, Figure 3 illustrates how modifying the trap distribution alters the profiles of the trapped charge, whilst maintaining a unique QFL profile. It is straightforward to appreciate that by increasing the trap density, the trapped charge will increase linearly. Decreasing the characteristic temperature of the distribution effectively biases it to have more states closer to the conduction band. This is why in Figure 3 the profile with a T_C value of 500K has fewer trapped electrons for the same QFL profile.

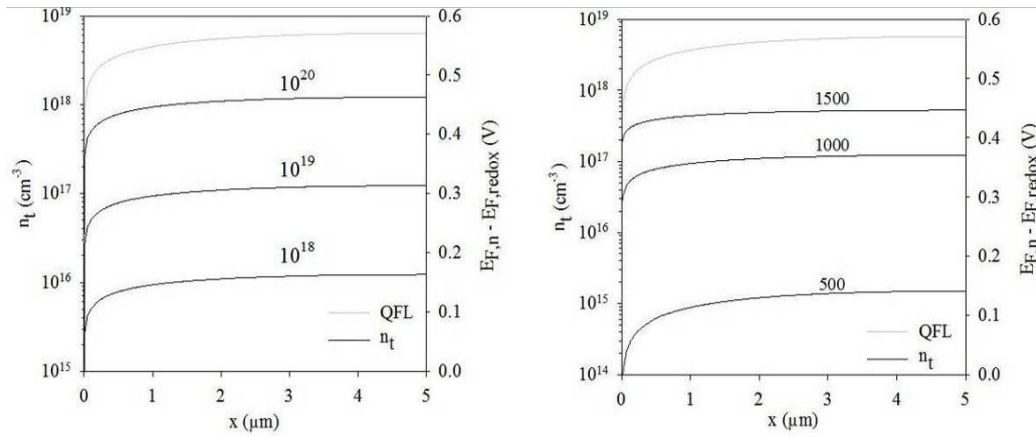


Figure 3 Effect of varying the total trap density N_t (left) and trap characteristic temperature T_C (right) on the trapped electron density, for an identical QFL profile at short-circuit. Standard parameters were: $D_0=0.04\text{cm}^2\text{s}^{-1}$, $\tau_0=1\text{ms}$, $E_C-E_{F,\text{redox}}=0.95\text{eV}$, $N_C=10^{21}\text{cm}^{-3}$, $N_t=10^{19}\text{cm}^{-3}$ (right), $T_C=1000\text{K}$ (left).

It is evident that there is an important link between the density of trapped electrons and the profile of the QFL. If there is no significant barrier to extraction at the FTO|TiO₂ interface, the measurements of the QFL only provide a measure of the QFL at two points, allowing one to infer the QFL between these two points. However, correlating the inferred QFL profiles with the trapped density for each inferred profile provides an interesting test of the applied models.

The basic concept to measure the stored charge along the iV curve, is to hold the cell at any point along the iV curve and to then simultaneously cease illumination and integrate the current output from the cell. However this has issues because of the timing between the cessation of illumination and switching to integration.

To circumvent the timing issues, modification were made to the PV decay charge extraction technique[6]. This apparatus was specifically designed to allow facile integration of small currents over long timescales. The cell was held at various points along the iV curve by adjusting the load by use of a resistor box (R_p). The small measuring resistor of the measuring apparatus was placed in parallel with the load resistance of the cell, but the switch would be closed only when integrating. Since the input resistance for the charge extraction kit is smaller than the load resistor, the discharge of the cell is faster, reducing integration times.

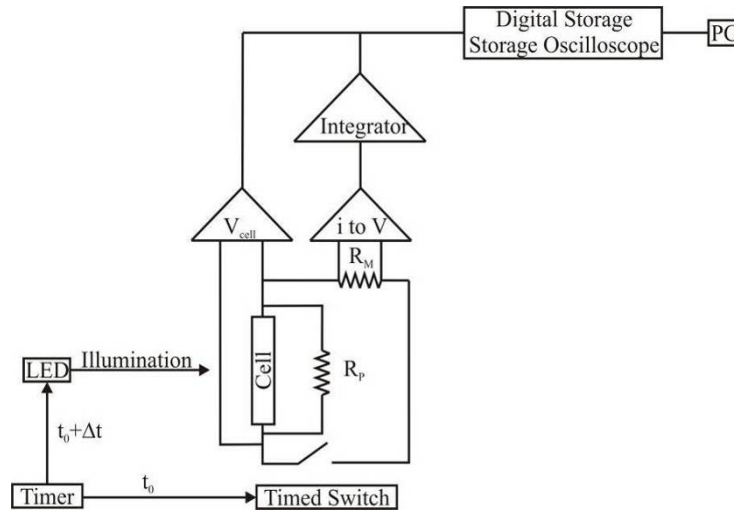


Figure 4: Schematic representation of how the charge extraction along the iV curve was measured.

Integration of current was initiated with the still cell in a photostationary state, i.e. still illuminated. The short time interval between short-circuiting the cell and cessation of illumination was well defined, so that the measured integrated charge before switching off the illumination could be subtracted from the total measured charge. As the cell was at short-circuit in this time interval, the extra photogenerated charge was assumed to be always equal. The extra integrated charge due to the time delay was also checked by careful numerical integration of the photocurrent decay profile at short-circuit (through a 10Ω resistor) and also by sequentially increasing the time delay and extrapolating back to a time delay of 0s. This was also crosschecked by the instantaneous square wave response of a photodiode acting in place of the cell. Once the integrator was initiated, the current from the cell would discharge through the two resistors in parallel. The fraction flowing through the measuring resistor was readily calculated in each case.

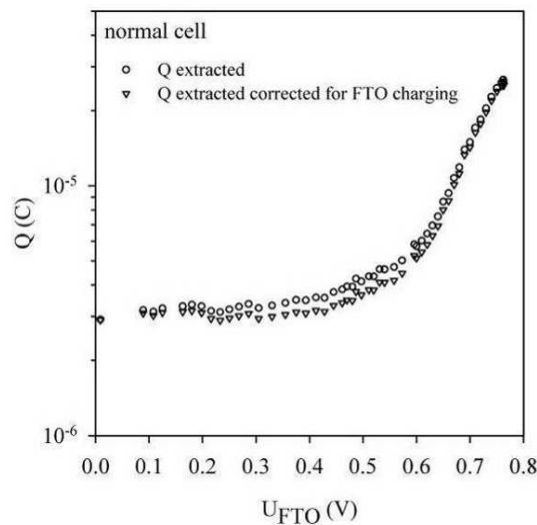


Figure 5 iV charge extraction data for a normal cell (left). The data shown are corrected for loss of current flow through the load resistor (R_p), and the extra integrated current due to the time delay $\Delta t=3.7\text{ms}$. An added correction for a hypothetical $Q=CV$ charging with $C=5\mu\text{Fcm}^{-2}$ ($1\mu\text{F}$ for the 0.196cm^2 cell) is also shown. The data points at $U_{FT0}\approx 0$ were obtained via numerical integration of the current decay transient and used as a crosscheck reference to correct for the extra integrated current. This resulted in an accuracy of 10% in the measured charge.

The general nature of the measured trapped electron density along the iV curves was as expected, whereby there was an inflection when the applied bias approached the short-circuit QFL inside the TiO_2 , c.a. 500mV. At this point, given that the QFL becomes homogeneous, further increase in the bias resulted in an exponential increase in measured charge (see figure in abstract).

Due to lack of full knowledge of the parameters defining electronic properties of the DSC, the uncertainty was translated to the parameters required to fit the experimental data.

For high potentials above the inflection point of c.a. 500mV, the fit is in excellent agreement with the data acquired from the normal cell. This is not surprising since for high potentials the QFL is homogeneous, and thus the measured charge is identical to that measured via open-circuit photovoltage decay charge extraction.

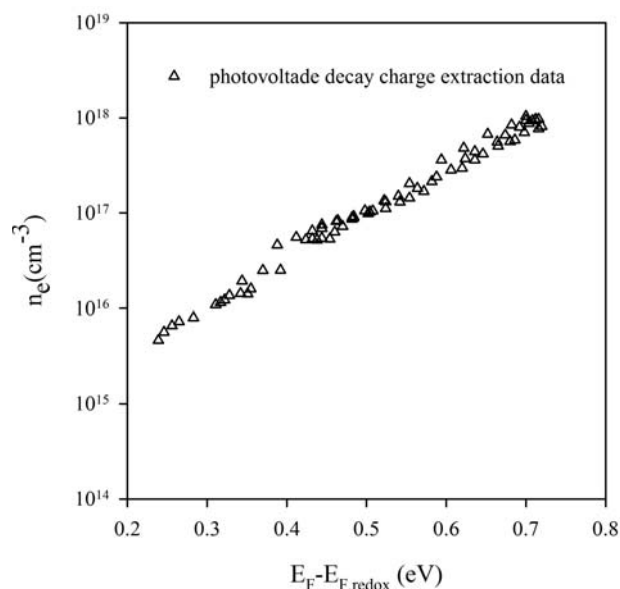


Figure 6 open-circuit photovoltage decay charge extraction data characterising the energetic trap distribution.

The inferred energetic (exponential) profile for the trap distribution may be incorrect. The uncertainty describing the trap distribution is only valid for the potential range through which the trap distribution is measured, where values below 300mV are difficult to determine. It could be possible that the trap distributions are not exponential at these lower potentials and any difference in their distribution would be more manifest at the lower potentials.

As for the uncertainty with the QFL measured at $x=5\mu\text{m}$, a difference in 30mV is enough to justify the extra trapped charge.

Although the modelled and experimental data relating the QFL and the trapped charge along the iV curve do not agree exactly, general trends were followed. These further confirm a large electron density and support a large electron density gradient within the TiO_2 film.

1. A.B. Walker, et al., *Analysis of photovoltage decay transients in dye-sensitized solar cells*. Journal of Physical Chemistry B, 2006. **110**(50) p.25504.
2. U. Würfel, J. Wagner, and A. Hirsch, *Spatial electron distribution and its origin in the nanoporous TiO_2 network of a dye solar cell*. Journal of Physical Chemistry B, 2005. **109**(43) p.20444.
3. B.C. O'Regan and F. Lenzmann, *Charge transport and recombination in a nanoscale interpenetrating network of n-type and p-type semiconductors: Transient photocurrent and photovoltage studies of $\text{TiO}_2/\text{Dye}/\text{CuSCN}$ photovoltaic cells*. Journal of Physical Chemistry B, 2004. **108**(14) p.4342.
4. G. Boschloo and A. Hagfeldt, *Activation energy of electron transport in dye-sensitized TiO_2 solar cells*. Journal of Physical Chemistry B, 2005. **109**(24) p.12093.
5. K. Lobato, L.M. Peter, and U. Würfel, *Direct measurement of the internal electron quasi-fermi level in dye sensitized solar cells using a titanium secondary electrode*. Journal of Physical Chemistry B, 2006. **110**(33) p.16201.
6. M. Bailes, et al., *Determination of the density and energetic distribution of electron traps in dye-sensitized nanocrystalline solar cells*. Journal of Physical Chemistry B, 2005. **109**(32) p.15429.
7. S. Sodergren, et al., *Theoretical-Models for the Action Spectrum and the Current-Voltage Characteristics of Microporous Semiconductor-Films in Photoelectrochemical Cells*. Journal of Physical Chemistry, 1994. **98**(21) p.5552.